GmSALT3 expression improves reactive oxygen species detoxification in salt-stressed soybean roots

Yue Qu[1], Lili Yu[2], Rongxia Guan[2], Oliver Berkowitz[3], Rakesh David[1], James Whelan[3], Melanie Ford[1], Stefanie Wege[1,*], Lijuan Qiu[2,*], Matthew Gilliham[1,*]

[1] ARC Centre of Excellence in Plant Energy Biology, Waite Research Institute & School of Agriculture, Food and Wine, University of Adelaide, Glen Osmond, SA, Australia

[2] The National Key Facility for Crop Gene Resources and Genetic Improvement, Institute of Crop Science, Chinese Academy of Agricultural Sciences, Beijing, China

[3] Department of Animal, Plant and Soil Science, School of Life Science, Australian Research Council Centre of Excellence in Plant Energy Biology, La Trobe University, Bundoora VIC 3083, Australia

[*]Correspondence should be addressed to:

Prof. Matthew Gilliham (matthew.gilliham@adelaide.edu.au)

Prof. Lijuan Qiu (qiulijuan@caas.cn)

Dr. Stefanie Wege (stefanie.wege@adelaide.edu.au)

Tel: +61 8 8313 8145

The date of submission:

The number of tables: 5

The number of Figure: 6

Word count: 4645

Supplementary data: 9 Figures and 1 Table

Running title: *GmSALT3*, ROS and salt-tolerance soybean

Highlight

RNA-seq analysis revealed that GmSALT3, which confers improved salt tolerance on soybean, improves reactive oxygen species detoxification in roots.

Abstract

Soybean plants are salinity (NaCl) sensitive, with their yield significantly decreased under moderately saline conditions. *GmSALT3* is the dominant gene underlying a major QTL for salt tolerance in soybean. *GmSALT3* encodes a transmembrane protein belonging to the plant cation/proton exchanger (CHX) family. It is currently unknown through which molecular mechanism(s) the ER-localised GmSALT3 contributes to salinity tolerance, as its localisation excludes direct involvement in ion exclusion. In order to gain insights into potential molecular mechanism(s), we used RNA-seq analysis of roots from two soybean NILs (Near Isogenic Lines); NIL-S (salt-sensitive, *Gmsalt3*) and NIL-T (salt-tolerant, *GmSALT3*), grown under control and saline conditions (200 mM NaCl) at three time points (0h, 6h, and 3 days). Gene ontology (GO) analysis showed that NIL-T has greater responses aligned to oxidation reduction. ROS were shown less abundant and scavenging enzyme activity was higher in NIL-T, consistent with the RNA-seq data. Further analysis indicated that genes related to calcium signalling, vesicle trafficking and Casparian strip (CS) development were upregulated in NIL-T following salt treatment. We propose that GmSALT3 improves the ability of NIL-T to cope with saline stress through preventing ROS overaccumulation in roots, and potentially modulating Ca^{2+} signalling, vesicle trafficking and formation of diffusion barriers.

Keywords: ROS; salinity tolerance; endomembrane; CPA2; *GmSALT3*; *GmCHX1; GmNcl*

Introduction

Plants use reactive oxygen species (ROS) as signalling molecules at low concentrations to control and regulate various biological processes, such as growth, programmed cell death, hormone signalling and development (Pei *et al.*, 2000; Mittler, 2002; Neill *et al.*; 2002, Foreman *et al.*, 2003; Overmyer *et al.*, 2003). However, ROS are also a toxic by-product of many reactions, which subsequently need to be eliminated by ROS scavenging enzymes. Under non-stressed conditions, the production of ROS and the capacity of the cell to scavenge them are generally at equilibrium (Foyer and Noctor, 2005). However, under biotic and abiotic stresses such as salinity, drought, temperature extremes, flooding, heavy metals, nutrient deprivation, and pathogen attack, intracellular ROS levels can increase dramatically. ROS at high concentrations damage plant cells through lipid peroxidation, DNA damage, protein denaturation, carbohydrate oxidation, and enzymatic activity impairment leading to significant damage to cellular functions and even cell death (Noctor and Foyer, 1998; Mittler *et al.*, 2004; Foyer and Noctor, 2005; Gill and Tuteja, 2010). ROS damage due to environmental stress is therefore a leading factor contributing to reduced global crop production. ROS have, for example, detrimental effects on membrane integrity under drought stress and cause early senescence, lowering crop yield (Mittler, 2002; Sharma *et al.*, 2017). In plants, ROS are eliminated through enzymatic and non-enzymatic pathways. Enzymatic antioxidant systems include scavenger enzymes such as SOD (superoxide dismutase), APX (ascorbate peroxidase), GPX (Glutathione peroxidases), PrxR (proxiredoxin), GST (glutathione-S- transferase), and CAT (Catalase); while non-enzymatic pathways include low molecular metabolites, such as ASH (ascorbate), GSH (glutathione), proline, α-tocopherol (vitamin E), carotenoids and flavonoids (Mittler *et al.*, 2004; Feroza *et al.*, 2016).

Among the above-mentioned stresses, salinity is one of the most prominent factors restricting crop production and agricultural economic growth worldwide. More than US$12 billion in revenue is estimated to be lost annually because of saline-affected agricultural land areas (Flowers *et al.*, 2010; Bose *et al.*, 2014; Gilliham *et al.*, 2017). Soybean (*Glycine max* (L.) Merrill) is an important legume crop that contributes 30% of the total vegetable oil consumed and 69% of human food and animal feed protein-rich supplements (Prakash, 2001; Lam *et al.*, 2010). The yield of soybean can be significantly reduced by salinity stress, especially during the early vegetative growth stage (Pi *et al.*, 2016).

In soybean, *GmSALT3* (also known as *GmCHX1* and *GmNcl*) has been identified as a dominant gene that confers improved salinity tolerance (Guan *et al.*, 2014; Qi *et al.*, 2014, Do *et al.*, 2016). It is mainly expressed in root phloem- and xylem-associated cells and the protein is localized to the ER (endoplasmic reticulum), not the plasma membrane (PM) (Guan *et al.*, 2014). NILs (near isogeneic lines), differing only in a transposon insertion in the *GmSALT3* gene, show that *GmSALT3* is involved in shoot exclusion of both, Na^+ (sodium) and Cl^- (chloride). In NIL-Ts with a functional GmSALT3, leaf Cl^- exclusion can be observed prior to Na^+ exclusion (Liu *et al.*, 2016), suggesting two distinct mechanisms for the exclusion of the two ions. Grafting of NILs showed that shoot Na^+ exclusion occurs via a root xylem-based mechanism and shoot Cl^- exclusion likely depends upon novel phloem-based Cl^- recirculation (Qu *et al.*, 2021). Additionally, *GmSALT3* is also related to K^+ homeostasis (Do *et al.*, 2016; Qu *et al.*, 2021). Despite the known importance of GmSALT3 for soybean salinity tolerance, the molecular mechanism through which the ER-localised GmSALT3 contributes to improved salinity stress tolerance has not yet been revealed.

There are studies providing a basis for examining the general responses of soybean roots to salt stress, however, these studies compared genetically diverse soybeans that differ in many aspects. High-throughput "-omics" technologies, including transcriptomics,

proteomics, and metabolomics have been applied in an attempt to understand soybean root responses to salinity stress (Aghaei *et al.*, 2009; Toorchi *et al.*, 2009; Ge *et al.*, 2010; Lu *et al.*, 2013; Qin *et al.*, 2013; Pi *et al.*, 2016). For instance, proteomic studies utilising the *Glycine max* cultivar Wenfeng07 (relatively salt-tolerant) and the *Glycine soja* (wild soybean) cultivar Union85-140 (relatively salt-sensitive), suggested that Wenfeng07's tolerance to salinity stress was associated with flavonoid accumulation in the tolerant accession. Flavonoids belong to the metabolites that scavenge ROS, and flavonoid synthesis is dependent on the activity of a few key enzymes, including chalcone synthase (CHS), chalcone isomerase (CHI) and cytochrome P450 monooxygenase (CPM) (Pi *et al.*, 2016). Wenfeng07 contains the *GmSALT3* salt tolerant allele and it is absent in Union85-140, but an explicit link between ROS detoxification, GmSALT3 and salt tolerance is not possible in this diverse genetic material.

We took advantage of our previously isolated NILs, and performed RNA-sequencing of NIL-T (salt-tolerant, *GmSALT3*) and NIL-S (salt-sensitive, *Gmsalt3*) roots, to further investigate the mechanism by which GmSALT3 confers salinity tolerance. Genes connected to ROS signalling were significantly differently regulated in NIL-T compared to NIL-S under saline conditions, suggesting a direct connection of ROS production to GmSALT3. Enzymatic assays further revealed that presence of *GmSALT3* is essential for maintaining ROS homeostasis under saline conditions. Differential gene expression under control conditions suggested that NIL-S might have a higher biotic resistance compared to NIL-T.

Materials and methods

Plant growth conditions and stress treatments

NIL-T (Salt-tolerant, *GmSALT3*) and NIL-S (Salt-sensitive, *Gmsalt3*) plants were grown in a growth chamber (RXZ-500D; Ningbo Jiangnan Instrument, China), with a day

length of 16h (with a light-emitting diode light source at 400 μmol m^{-2} s^{-1}) at 28 ˚C, and 8 h dark at 25 ˚C, with 60% relative humidity throughout. Soybean seedlings were treated with 200 mM NaCl (salt treatment) or water (control) at 10 days after sowing (DAS). 200 mM NaCl or water were applied again at 12 DAS.

Total RNA extraction and RNA-seq library construction

Total RNA was extracted from soybean roots using TRIZOL reagent (Ambion, http://www.ambion.com). Root samples were harvested at three time points, 0h, 6h, and 3d of a 200 mM salt-treatment with the corresponding non-treatment controls. To remove the residual DNA, the extracted RNA was treated with RNase-free DNase I (New England Biolabs, https://www.neb.com) for 30 min at 37°C. Thirty RNA libraries were generated for paired-end reads using an Illumina HiSeq 2500 sequencer, consisting of 3 biological samples per time point per genotype.

RNA-seq data analysis and assembly

Raw reads were generated and mapped to the latest soybean genome sequence Gmax_275 Wm82.a2.v1 (Glyma 2.0) using TopHat2 (Kim *et al.*, 2013). Clean mapped reads were obtained by removing low quality (Q<30) sequences, adapter fragments and barcode sequences. A quality control test by fastQC (Andrews, 2010) revealed the quality of RNA-seq libraries construction and sequence alignment were sufficient for further analysis.

Gene expression level and DEG analysis

Gene expression was compared in FPKMs (Fragments Per Kilobase of transcript per Million) calculated using the Cufflinks functions cuffquant and cuffnorm (Trapnell *et al.*, 2012). Differential expression analysis of two conditions/groups was performed using the

149 DESeq R package (1.10.1). The resulting P values were adjusted using the Benjamini and
150 Hochberg's approach for controlling the false discovery rate. The cut-offs for differentially
151 expressed genes (DEGs) were Log_2FC (fold change) ≥ 1, FDR (False Discover Rate) < 0.01.
152
153 *GO enrichment and KEGG pathway analysis*
154 GO enrichment analysis of DEGs was implemented using AgriGO (Du *et al.*, 2010).
155 GO terms with corrected *p* values < 0.05 were deemed significantly enriched. KEGG
156 (Kanehisa *et al.*, 2007) is a database resource for understanding high-level functions and
157 utilities of the biological system, such as the cell, the organism and the ecosystem, from
158 molecular-level information, especially large-scale molecular datasets generated by genome
159 sequencing and other high-throughput experimental technologies
160 (http://www.genome.jp/kegg/). We used KOBAS (Mao *et al.*, 2005) software to test the
161 statistical enrichment of differential expression genes in KEGG pathways.
162
163 *Weighted Gene Co-expression Network Analysis (WGCNA)*
164 There were 54,175 genes annotated in all the RNA-seq libraries. After filtering out
165 non-expressed genes, low-expressed genes (FPKM < 2) and genes that possessed large
166 expression variation across replicates, 28,223 genes were selected for WGCNA analysis. An
167 unsigned gene co-expression network was built using the WGCNA R-package (Langfelder
168 and Horvath, 2008). The Topological Overlap Measure (TOM) was calculated using the
169 adjacency matrix between all genes with a power of 18. A gene dendrogram was created by
170 using the dissimilarity TOM. Branches of the dendrogram (Supplementary Fig. 6) indicated
171 modules (clustered highly co-expressed genes) through using the Dynamic Tree Cut
172 algorithm (Langfelder et al., 2008). Each module has an assigned colour. Similar modules
173 were merged by calculating module eigengenes. Using the module eigengenes, the Module –

Trait Relationships (MTRs) were plotted by calculating the Pearson's correlations between the module eigengene and the samples (traits). A correlation of 0.75 with at least one of the selected traits was the criteria used to generate modules. Clustered genes in modules of interest were then used for further analysis. Genes annotation and GO term analysis were performed in Soybase (Grant *et al.*, 2010) and AgriGO (Du *et al.*, 2010), respectively.

ROS production and contents measurement

Fourteen-day-old NIL-T and NIL-S soybean seedlings were used to measure the generation of ROS in roots. Roots were labelled with 30 μM Dichlorofluorescein diacetate (DCFDA; Sigma-Aldrich, USA), by incubating washed soybean roots for 10 min at room temperature in the dark with 30 μM DCFDA. ROS sensitive fluorescent dyes were imaged using a Nikon SMZ25 stereo microscope (Nikon, Japan). The excitation and emission wavelengths were 488 nm and 500/535 nm, respectively.

ROS contents in soybean root samples were measured using Amplex® UltraRed reagent (Invitrogen, USA). Sodium phosphate buffer (0.5 ml 50 mM pH 7.4) was added to 0.1g soybean powder, after mixing and solubilisation, samples were set on ice for 5 min. Then tubes were centrifuged at 12 x 1000 g for 20 min. 500 μl supernatant was transferred into new tubes. An equal volume of 2:1 (v/v) chloroform : methanol was added and centrifuged at 12 x 1000 g for 5 min. 50 μl aqueous phase was took from each sample and add into each well of 96-well microplate. 50 μl working solution (freshly made) was added into each well. Plates were incubated at 25 °C for 30 min (protected from light). Fluorescence was measured at 540/590 nm.

Scavenging activity of the superoxide anion (O_2^-) assay

The scavenging activity assay was adapted from Pi *et al.* (2016) with slight modifications. Less root homogenate (0.1 g) was used for measurement. Antioxidant enzymes were extracted with 2 ml of 0.05 M phosphate buffer (pH5.5) from 0.1 g root homogenate. The extract was then centrifuged at 12,000 x g (4 ℃) for 10 min. Supernatant (40 µl) was added into 160 µl reaction buffer, which contains 80 µl phosphate buffer, 40 µl 0.05 M guaiacol (Sigma, USA), 40 µl 2% hydrogen peroxide (H_2O_2). The increased absorbance at 470 nm in 96-well plates due to the enzyme-dependent guaiacol oxidation was recorded every 30s until 4 min of reaction.

Real-time quantitative reverse-transcription polymerase chain reaction (RT-qPCR) validation for RNA-seq results

Total RNA was extracted from soybean root tissues using TRIZOL reagent (Ambion, http://www.ambion.com). To remove the residual DNA, the extracted RNA was treated with RNase-free DNase I (New England Biolabs, https://www.neb.com) for 30 min at 37°C. For gene expression, first-strand cDNA synthesis was done with a PrimeScript RT Reagent Kit (TaKaRa, Japan, http://www.takara.co.jp/english). Real-time PCR was performed using SYBR Premix Ex Taq II (TliRNaseH Plus) (TaKaRa). The level of *GmSALT3* transcript was normalised using the control gene *GmUKN1* (Hu *et al.*, 2009).

Results

RNA-sequencing preparation and profiles

GmSALT3 has previously been shown to be expressed in roots, and grafting experiments have shown that presence of GmSALT3 expression in roots is sufficient to confer shoot Na^+ and Cl^- exclusion (Guan *et al.*, 2014; Qu *et al.*, 2021). Total root RNA was extracted from NIL-T and NIL-S, and transcriptomes obtained using RNA-seq in a time

course from plants grown under control and saline conditions. To investigate short- and long-term responses, root samples were harvested at three time points, 0h (control), 6h, and 3d with 200 mM salt-treatment and controls (Fig. 1a; 1b) and in biological triplicates. Thirty RNA libraries were generated for paired-end reads using an Illumina HiSeq 1500 sequencer. In total, 1.6 billion paired 100 bp raw reads were generated and mapped to the soybean genome sequence Gmax_275 Wm82.a2.v1 (Glyma 2.0) using TopHat2 (Kim *et al.*, 2013). The average mapping percentage was 81.25%. After trimming of low quality (Q<30), adapter fragments and barcode sequences, a total of 804 million clean mapped reads were identified. Combined with a quality control test using fastQC (Andrews, 2010), the quality of RNA-seq libraries construction and sequence alignment was deemed sufficient for further analysis. A summary of mapped reads and quality of sequencing is shown in Table 1. Transcripts corresponding to *GmSALT3/Gmsalt3* in the NIL-T and NIL-S in all samples were confirmed. NIL-T transcriptomes contained reads across the entire full-length transcript for *GmSALT3* were obtained, while in NIL-S reads only mapped to the predicted truncated version *Gmsalt3* (Fig. 1c). A flowchart of data analysis is shown in Fig. 1d.

Overview of DEGs between NIL-T and NIL-S under control conditions

Previous work had shown that *GmSALT3* is expressed under both control and saline conditions, suggesting that there might already be a difference in other gene expression between NIL-T and NIL-S under control conditions. We therefore first compared the transcriptomes of NIL-T and NIL-S (indicated as “T” and “S”, respectively) under control conditions, before analysing changes due to salinity treatment. A PCA plot (for the first two principal components) of ten grouped samples shows a good separation between all comparisons, confirming replicates clustered together consistently. Those comparisons are: Control 0h T vs Control 0h S (grey), Control 3d T vs Control 3d S (purple), and Control 6h T

vs Control 6h S (brown) (Fig. 2a). There are 5 up-regulated Differentially Expressed Genes (DEGs) at 0h, 9 up-regulated DEGs at 6h, and 6 up-regulated DEGs at 3d in NIL-S (compared to NIL-T), and a Venn diagram demonstrates 3 of these genes are common across three time points. There were 1, 5, and 5 down-regulated DEGs at 0h, 6h, and 3d, respectively, but the identity of the down-regulated DEGs were different between each of the time point (Fig. 2b). The three consistently up-regulated DEGs in NIL-S at all time points under control conditions were *Glyma.07G196800* (Linoleate 13S-lipoxygenase 3-1), *Glyma.10G143600* (uncharacterized protein), and *Glyma.20G105500* (3-hydroxybenzoate 6-hydroxylase 1-like) (Fig. 2c). Fig. 2d shows the expression profile (in FPKM, Fragments Per Kilobase of transcript per Million) of these three genes at all time points of NIL-T and NIL-S under control conditions.

Overview of DEGs in salt treated NIL-T and NIL-S when compared to their respective controls

Transcript abundance was compared in FPKMs calculated using the Cufflinks functions cuffquant and cuffnorm (Trapnell *et al.*, 2012). DEGs were classified as genes with a Log_2FC (fold change) ≥ 1 and a FDR (False Discover Rate) < 0.01 when comparing between two conditions. Gene expression differences in response to salt of each genotype was examined separately; to identify the DEGs in NIL-T and in NIL-S in response to salt. Using these parameters and comparing control to salt treated NIL-T, we identified 1816 DEGs that were differently expressed in NIL-T roots in response to salt (1263 up-regulated and 553 down-regulated, 6h T).

We then did the same analysis for NIL-S roots, and compared expression of control and salt treated NIL-S. 6h salt treated NIL-S roots (when compared to control NIL-S) showed a greater initial response in term of DEGs than we found in NIL-T, with a total of 3054 DEGs

(1911 up-regulated and 1143 down-regulated, 6h S) (Fig. 3b). After three days of salt treatment, the increased number of DEGs in NIL-S was not observed anymore. On the contrary, the NIL-T now showed a slightly higher number of DEGs compared to control conditions. Now, the NIL-T had 2844 DEGs (1333 up-regulated and 1511 down-regulated, 3d T) while there were 2573 DEGs (1318 up-regulated and 1255 down-regulated, 3d S) in NIL-S roots (Fig. 3b).

Hierarchical clustering of the DEGs of the three replicates in different grouped samples is shown in Fig. 3c-f. These DEGs represent the genes that each soybean line up- or downregulates in response to salt. We then used the hierarchical clustering to identify DEGs, which either similarly change in expression in the two genotypes in response to salt, and which genes show a different change in expression comparing the two genotypes. Analyses of the similarities and differences between the tolerant and sensitive lines indicated that 341 and 989 DEGs are uniquely up-regulated after 6h salt treatment in NIL-T or NIL-S, respectively; and 608 and 593 in the 3d salt treatment, respectively (Fig. 3g). We found similar values for uniquely down-regulated DEGs (Fig. 3h).

GO analysis of DEGs between control and salt-treated samples of NIL-T and NIL-S

To gain insight into the putative functions of the uniquely up- and down-regulated DEGs at 6h salt treatment, the identified genes were subjected to GO (Gene Ontology) enrichment analysis, the representative GO terms are shown in Table 2, and detailed GO terms are shown in Supplementary Fig. 1 - 4.

The enriched GO terms for the 6h T (NIL-T) up-regulated DEGs were all related to stress response such as “oxidation reduction”, “defence response” and “response to biotic stimulus” (Table 2a). Down-regulated GO terms in NIL-T were less specific and mainly associated with “integral to membrane” (Table 2c). For 6h S (NIL-S), a large number of up-

298 regulated genes were associated with the very broad GO term "regulation of transcription,
299 DNA-dependent (GO:0006355)", and no further downstream classification was considerably
300 enriched (Table 2b). Down-regulated GO terms in NIL-S included "heme binding", "electron
301 carrier activity", "aspartic-type endopeptidase activity", and "protein disulphide
302 oxidoreductase activity" (Table 2d), relating to protein types instead of specific biological
303 process GO terms.

304 After 3 days of salt treatment, GO analysis of uniquely up- and down-regulated DEGs
305 showed that only "oxidation reduction" and "oxidoreductase activity" were up-regulated in
306 NIL-T (Table 3a). "Oxidation reduction" and "oxidoreductase activity" were consistently up-
307 regulated in NIL-T at both time points. Table 4 shows all the 53 up-regulated genes in
308 "oxidation reduction" and "oxidoreductase activity" GO terms after 3d treatment in NIL-T
309 roots. A group of Cytochrome P450 enzymes-encoding genes were significantly more highly
310 expressed in NIL-T, especially *Glyma.13G173500*, which had a FPKM of 279 compared to
311 71 under control conditions (Table 4). Other genes encoding oxidoreductase enzymes were
312 also included such as peroxidases and dehydrogenases (Table 4). All the gene annotations in
313 each GO are shown in Supplementary Table 1.

314

315 *KEGG analysis of DEGs between control and salt-treated samples*

316 To understand what pathways were differently altered in NIL-T and NIL-S under salt
317 stress, KEGG (Kyoto Encyclopedia of Genes and Genomes) analysis was performed. This
318 analysis can reveal enrichments of biological pathways, similar to GO term analysis but
319 KEGG takes fold changes of DEGs into account, while the GO term analysis does not.

320 In our analysis, 1816 and 3054 DEGs in NIL-T and NIL-S, respectively, were
321 enriched in 58 pathways (corrected p-Value <0.05) after 6h salt-treatment (Fig. 4a). Most of
322 the 58 pathways in both NIL-T and NIL-S were within the metabolism category with

323 "Phenylpropanoid biosynthesis", "Phenylalanine metabolism", and "Starch and sucrose
324 metabolism" as the top three pathways (Fig. 4a). Overall, NIL-S has more DEGs compared to
325 NIL-T after salt-treatment, across all significantly changed pathways.

326 After three days of salt stress (3d), 2844 and 2573 DEGs in NIL-T and NIL-S,
327 respectively, were mapped to 57 pathways (corrected *p*-Value <0.05) (Fig. 4b). The
328 metabolism category was also the most enriched after 3 days with similar pathways involved
329 compared to 6 hours. After 3d salt-treatment, most of the significantly changed pathways
330 included more DEGs in NIL-T compared to NIL-S, in particular in the pathway "Protein
331 processing in endoplasmic reticulum" (16 to 11 DEGs), the cell organelle where GmSALT3
332 is localised (Guan *et al.*, 2014). DEG enrichment in NIL-T was also higher in the pathways
333 "Ubiquitin mediated proteolysis" (10 to 3 DEGs), "Phenylpropanoid biosynthesis" (71 to 60
334 DEGs), "Phenylalanine metabolism" (52 to 42 DEGs), "Starch and sucrose metabolism" (43
335 to 35 DEGs), and "Plant-pathogen interaction" (33 to 20 DEGs). It is important to note that
336 all plants (NIL-T and NIL-S) were grown together and no plants showed signs of infection,
337 suggesting that the genes categorised into this pathway also have a function in abiotic stress
338 response.

339 In the "Plant-pathogen interaction" pathway, the putative CNGC (Cyclic Nucleotide-
340 Gated ion Channel) 15-like gene, *Glyma.13G141000*, was significantly down-regulated in 3d
341 T (Supplementary Fig. 5a; 5b), probable putative CNGC 20-like gene, *Glyma.09G168700*,
342 was upregulated in 3d S. Several CaM (Calmodulin) and CML (Calmodulin-like) genes were
343 down-regulated in 3d T. CDPK (Calcium-Dependent Protein Kinase 3, *Glyma.08G019700*)
344 and Rboh (Respiratory Burst Oxidase Homolog protein F-like isoform 1, *Glyma.01G222700*)
345 were up-regulated in 3d S. However, at 6h, another CNGC 20-like gene (*Glyma.16G218300*),
346 homolog to the Arabidopsis putative Ca^{2+} channel that is proposed to regulate cytosolic Ca^{2+}

activity and expression of Rhob and CaM/CML (Demidchik *et al.*, 2018), was significantly up-regulated in NIL-T (Supplementary Fig. 5d).

Weighted Gene Co-expression Network Analysis (WGCNA)

WGCNA identifies genes that have strongly correlated expression profiles, and those genes work cooperatively in related pathways to contribute to corresponding phenotypes. It is based on the concept that genes with strongly correlated expression profiles are clustered because those genes work associatively in related pathways, contributing to the resulting phenotype; in our case, establishing salinity tolerance after salt treatment. We applied the WGCNA to the normalized FPKM data (FPKM > 2) from all 30 RNA-seq libraries.

A co-expression network was constructed, and highly co-expressed genes were assigned to different colour-coded modules (Supplementary Fig. 6). Clusters were summarized by correlating the module's eigengene (or an intromodular hub gene) to the sample traits (Langfelder and Horvath, 2008). Module - Trait Relationships (MTRs) were computed based on Pearson's correlation between module and phenotypes, and then be used to screen modules for downstream analysis. Thirty clusters of highly co-expressed genes (modules) were detected and are shown in differently coloured module (Fig. 5). To investigate what genes show strongly correlated co-expression in NIL-T under saline conditions (6h and 3d), two modules of interest were selected for functional annotation based on their correlation value and corresponding *p*-Value. One module contains 79 genes that show strongly correlated co-expression in NIL-T after 6h salt treatment; this model is depicted here in a shade of pink (MEdeeppink). The second selected module, colour-coded here in a shade of white (MEantiquewhite2), contains 406 genes which expression profiles are highly correlated in NIL-T after 3d salt treatment.

GO analysis of 79 genes in module MEdeeppink is shown in Table 5a; GO analysis of 406 genes in module MEantiquewhite2 is shown in Table 5b. Within the highly co-expressed 79 genes in NIL-T after 6h salt treatment (MEdeeppink module), Gene Ontology (GO) analysis indicates 12 of them are integral to plasma membrane (GO:0016021; Table 5a), and they encode a group of Casparian strip membrane proteins (Supplementary Table 1). Highly co-expressed 406 genes in NIL-T after 3d salt treatment (MEantiquewhite2 module) are enriched in GO: 0016021 (integral to membrane; 26 genes), which are related to intracellular vesicle trafficking and ion transport (Table 5b). Within those GOs, there are genes relevant to vesicle transport, such as genes encoding for coatomer subunits and transmembrane protein transporters; three potassium transporters including Glyma05g37270 (TRH1; tiny root hair 1), Glyma08g39860 (KUP6; potassium ion uptake transporter 6), and Glyma13g23960 (Supplementary Table 1).

RT-qPCR validation for RNA-seq results

In order to confirm the RNA-seq results, 10 DEGs were selected for RT-qPCR validation based on their RPKM transcript abundance. Importantly, this occurred on independently grown plants not used for RNAseq analysis but grown in identical conditions. RT-qPCR indicated that relative expression values (relative to housekeeping gene *GmUKN1*) of the selected DEGs were significantly correlated with their FPKM values (supplementary Fig. 7).

ROS production and scavenger enzymes activity

Due to the enrichment of the “Oxidation reduction” gene ontology category in NIL-T plants under salt (Table 4), we decided to test if this translated into a difference in ROS generation or detoxification in NIL-T compared to NIL-S, again on independently grown

plants. The ROS activity was measured in the roots of NIL-T and NIL-S after a 3-day treatment with or without salt treatment, using a fluorescent dye (Fig. 6a; 6b). We could detect a lower ROS activity in NIL-T compared to NIL-S roots, already in the control conditions, consistent with the expression of *GmSALT3* under control conditions. This difference strongly increased when comparing plants from saline conditions; ROS were strongly produced in NIL-S under salt treatment.

ROS are composed of many different molecules; we initially measured the concentration of the ROS H_2O_2. We could detect a higher H_2O_2 concentration in both lines under salt treatment compared to control; but no concentration differences between NIL-T and NIL-S in either control or salt treatment could be measured (Supplementary Fig. 9), suggesting that the increase in ROS is attributed to a different molecule. The antioxidant properties of the roots of NIL-T and NIL-S with or without salt treatment was then analysed using guaiacol. The antioxidant enzyme activity was assayed by measuring the absorbance at 470 nm due to the enzyme dependent oxidation of guaiacol by H_2O_2 (Pi *et al.*, 2016). The scavenging enzyme activity of the superoxide anion was significantly higher in NIL-T compared to NIL-S under control and saline conditions (Fig. 6c).

Discussion

Soybean cultivars harbouring *GmSALT3* are better able to modulate Na^+, K^+, and Cl^- content of shoots under salinity (Guan *et al.*, 2014; Qi *et al.*, 2014; Do *et al.*, 2016; Liu *et al.*, 2016; Qu *et al.*, 2021), and they have a yield advantage under saline conditions compared to soybean varieties without a functional *GmSALT3* (Do *et al.*, 2016, Liu *et al.*, 2016). The GmSALT3 ion transport protein is ER-localised (Guan *et al.*, 2014), suggesting a cellular function of GmSALT3 that is not directly connected to ion uptake or exclusion. We performed detailed and extended RNAseq analysis of NIL-T and NIL-S soybeans to decipher

the cellular pathways and processes that connect *GmSALT3* to soybean salinity tolerance. We could identify several genes and biological pathways involved in responses to salt stress in *GmSALT3*-containing NIL-T plants, which gives an insight into how *GmSALT3* expression translates into a phenotype thorough modulating cell processes.

Illumina sequencing results showed that all the 30 constructed RNA-seq libraries were of sufficient quality for further analysis. On average the RNA-seq libraries had 26.8 million clean mapped reads, and reads were mapped to 53,625 annotated soybean genes with 353 additional transcripts not previously annotated – probably due to the germplasm being genetically divergent from the reference. Minimal DEGs could be detected between NIL-T and NIL-S at 0h, 6h, and 3d under control conditions (Fig. 2), this indicates that NIL-T and NIL-S roots had similar gene expression patterns under non-stressed conditions. In the three consistently up-regulated DEGs in NIL-S at all time points under control conditions, there was a gene encoding for a LOX (Linoleate 13S-lipoxygenase 3-1) (Fig. 2c). Lipoxygenases (LOXs) are involved in defence responses against biotic stresses, such as microbial pathogens and insect pests, in tomato (Hu *et al.*, 2015), potato (Royo *et al.*, 1999), maize (Gao *et al.*, 2009), and rice (Zhou *et al.*, 2009). The full length *GmSALT3* during soybean natural selection and domestication was lost several times independently (Guan *et al.*, 2014), suggesting that plants with a non-functional GmSALT3 might have a benefit when grown under non-saline conditions. This benefit might be related to higher LOXs expression in soybean cultivars harbouring the sensitive alleles, which could be beneficial under certain biotic stresses. In potato, depletion of one specific LOX (LOX-H3) negatively affected their response to stress (Royo *et al.*, 1999), but here in soybean, plants with the full length *GmSALT3* had lower LOX expression than with the non-functional GmSALT3. Therefore, this calls for further research to investigate the role of these LOX in soybean function and whether there is a link to GmSALT3 in response to abiotic stresses in soybean.

Comparing DEGs, the GO terms "Oxidation reduction (GO:0055114)" and "oxidoreductase activity (GO:0016491)" were consistently up-regulated in NIL-T at 6h and 3d of salt treatment, with a greater number of genes in this term up-regulated after 3 days, which indicates that NIL-T plants may have a greater capacity to detoxify ROS (Reactive oxygen species) than NIL-S plants. We could experimentally confirm this and show that more ROS is produced NIL-S compared to NIL-T (Fig. 6a; 6b) and NIL-T possessed a significantly higher scavenging enzyme activity of the superoxide anion (O_2^-) (Fig. 6c). Phenylalanine is the precursor for flavonoids, and flavonoids are utilised to scavenge and protect against ROS (Dastmalchi *et al.*, 2016). The increase in gene expression related to phenylalanine synthesis seen in NIL-T (Fig 4a; 4b) is consistent with the observation that GmSALT3 is connected to an increase in general ROS detoxification capacity.

In all the listed up-regulated genes in NIL-T (Table 4), a group of Cytochrome P450 enzymes-coding genes were significantly more highly expressed in NIL-T in response to salt-treatment, especially *Glyma.13G173500,* which has the highest expression level and a fold change of 3.93. The cytochrome P450 (CYP) family is a large and essential protein superfamily in plants, and CYPs catalyse monooxygenation/hydroxylation reactions in primary and secondary metabolism pathways (Mizutani and Ohta, 2010). NaCl can induce conformational change of cytochrome P450 in animals (Yun *et al.*, 1996; Oyekan *et al.*, 1999), but this has not been investigated in plants. In soybean, there are 322 identified CYPs, with only few of them having been functionally characterised (Guttikonda *et al.*, 2010). *GmCYP82A3* (*Glyma.13g068800*) (Yan *et al.*, 2016) and *GmCYP51G1* (*Glyma.07g110900*) (Pi *et al.*, 2016) were shown to be involved in plant tolerance stresses such as salinity and drought. The two P450 containing isoflavone synthases (IFS) *GmIFS1* (*Glyma.07G202300*) and *GmIFS2* (*GmCYP93C1 = Glyma.13G173500*) are both anchored in the ER, the same organelle where GmSALT3 is localised. *GmIFS2* is a DEG identified in our study.

Expression of *GmIFS1* was previously shown to be induced by salt stress, and has been linked to improving salinity tolerance through the accumulation of isoflavone content (Jia *et al.*, 2017). We found its homologue, *GmIFS2* (*Glyma.13G173500)*, had a fold change of 3.93 in NIL-T in response to salt stress (Table 4). Combined, this suggests that the function of GmSALT3 could be important for the synthesis of isoflavones, and this may contribute to salt tolerance.

ROS production has been linked to Ca^{2+} influx into cells and specifically the activity of CNGCs (Ma *et al.*, 2009). Ca^{2+} and ROS act as signalling molecules when plant roots are suddenly exposed to salt (Byrt *et al.*, 2018). Gene expression related to proposed Ca^{2+} signalling elements are different between NIL-T and NIL-S. As a result, our analysis suggested that the "Plant-pathogen interaction" pathway could be highly activated in NIL-S, which may lead to higher ROS production and hypersensitive responses (Supplementary Fig. 5a; 5c). Under 6h salt treatment, several CNGCs were also significantly up-regulated in NIL-S, which may relate to activation of different signalling cascades (Supplementary Fig. 5d). Several CaM (Calmodulin) and CML (Calmodulin-like) genes are also down-regulated in 3d T (Supplementary Fig. 5b), down-regulation of CaM and CML may has been proposed to restrict gaseous reactive oxygen species (ROS) production in plants (Ma and Berkowitz, 2011).

The WGCNA analysis revealed that genes related to Casparian strip (CS) development were upregulated in NIL-T within 6 hours of salt treatment. CSs play an important role in regulating nutrient uptake and salt stress tolerance, as they form the diffusion barrier for ions into the stele (Chen *et al.*, 2011; Roppolo *et al.*, 2011). CS localised membrane proteins (CASPs) were shown to mediate CS formation in Arabidopsis, by guiding the local lignin deposition during cell wall modification (Roppolo *et al.*, 2011). Upon immobilisation, CASPs recruit PER64 (Peroxidase 64), RBOHF (Respiratory Burst Oxidase

Homolog F), ESB1 (Enhanced Suberin 1), and dirigent proteins, to establish the lignin polymerization system (Hosmani et al., 2013; Kamiya et al., 2015; Lee et al., 2013). Our analysis identified a module of genes upregulated under salt exclusively in the NIL-T (MKdeeppink module). This module contains 8 dirigent genes, peroxidase 64 (Glyma.14g221400) as well as CASPs. The combination of genes in this model suggests that NIL-T plants might more efficiently induce an earlier formation of the endodermal diffusion barrier as well as the formation of an exodermal diffusion barrier, in response to salt stress. We stained lignin and suberin in NIL-T and NIL-S roots with ClearSee and Auramine O, following the protocol developed by Ursache *et al.* (2018), in order to compare the CS development. Unfortunately, we could only observe autofluorescence in both NIL-T and NIL-S root differentiation zone that close to the root tips using confocal microscopy. So the link between GmSALT3 and CS formation needs further validation.

Lastly, CHX transporters (of which GmSALT3 is a member) were shown to be associated with the endocytic and exocytic pathways in dynamic endomembrane system (Chanroj *et al.*, 2012; Padmanaban *et al.*, 2007). Our results and the previously proposed vesicle trafficking function of CHXs (Chanroj *et al.*, 2012), suggests that GmSALT3 might be important for establishing optimal conditions in the ER lumen, which could subsequently impact the secretion of compounds such as signalling molecules, ions, and soluble proteins.

To summarize, our findings suggest that the GmSALT3 containing NIL-T has a higher salinity tolerance because NIL-T roots are more effective in scavenging ROS, which helps to prevent cellular damage. Our results suggest that the improved ROS detoxification mechanisms might be connected to ER-localised flavonoid biosynthesis enzymes. Additionally, our study has identified that Ca^{2+} signalling, vesicle trafficking and Casparian strip development might be modulated by GmSALT3, and are therefore areas for further study.

Supplementary data

Supplementary Fig. 1 GO term analysis of unique DEGs under salt treatment in NIL-T roots after 6h 200 mM NaCl treatment.

Supplementary Fig. 2 GO term analysis of unique DEGs under salt treatment in NIL-S roots after 6h 200 mM NaCl treatment.

Supplementary Fig. 3 GO term analysis of unique DEGs under salt treatment in NIL-T roots after 3d 200 mM NaCl treatment.

Supplementary Fig. 4 GO term analysis of unique DEGs under salt treatment in NIL-S roots after 3d 200 mM NaCl treatment.

Supplementary Fig. 5. DEGs between salt-treated and control samples of NIL-T and NIL-S in plant-pathogen interaction KEGG pathway at 6h and 3d.

Supplementary Fig. 6 Gene dendrogram showing the co-expression modules defined by the WGCNA labelled by colours.

Supplementary Fig. 7 qPCR validation for RNA-seq results of selected genes.

Supplementary Fig. 8 *Glyma.13G173500* (*GmIFS2*) gene expression (FPKM) in all samples.

Supplementary Fig. 9 H_2O_2 concentration measurement in soybean roots.

Supplementary Table 1 gene annotations in each GO (attached as an Excel file).

Acknowledgements

This work was funded by the Natural Science Foundation of China, grant number 31830066 (RG); Scientific Innovation Project of Chinese Academy of Agricultural Sciences (L-J Q). YQ and SH were supported by ARC Centre of Excellence funding awarded to MG (CE140100008). ARC Fellowships supported MG (FT130100709) and SW (DE160100804). We thank Na Sai and Dr. Miriam Schreiber for assisting in WGCNA analysis.

Author contributions

MG, YQ and RG designed experiments, with input from SW and LQ. YQ and RG analysed the data. LQ and MG directed the project. OB and JW contributed to RNA-sequencing. LY performed plant samples harvest for RNA-sequencing. RD contributed to RNA-sequencing analysis. YQ, MG and RG wrote the paper. SW and LQ assisted in editing the final version of the manuscript. All authors commented on the manuscript.

Conflict of interest

The authors declare that they have no conflict of interest.

Data availability statement

The data supporting the findings of this study are available from the corresponding author, Matthew Gilliham, upon request.

References

Aghaei K, Ehsanpour A, Shah A, Komatsu, S. 2009. Proteome analysis of soybean hypocotyl and root under salt stress. Amino Acids **36**, 91-98.

Andrews S. 2010. FastQC: a quality control tool for high throughput sequence data. http://www.bioinformatics.babraham.ac.uk/projects/fastqc/.

Bose J, Rodrigo-Moreno A, Shabala, S. 2014. ROS homeostasis in halophytes in the context of salinity stress tolerance. Journal of Experimental Botany **65**, 1241-1257.

Byrt CS, Munns R, Burton RA, Gilliham M, Wege S. 2018. Root cell wall solutions for crop plants in saline soils. Plant Science **269**, 47-55.

Chanroj S, Wang G, Venema K, Zhang MW, Delwiche CF, Sze H. 2012. Conserved and diversified gene families of monovalent cation/H^+ antiporters from algae to flowering plants. Frontiers in Plant Science **3**, 25.

Chen T, Cai X, Wu X, Karahara I, Schreiber L, Lin J. 2011. Casparian strip development and its potential function in salt tolerance. Plant signaling & behavior **610**, 1499-1502.

Dastmalchi M, Bernards MA, Dhaubhadel S. 2016. Twin anchors of the soybean isoflavonoid metabolon: evidence for tethering of the complex to the endoplasmic reticulum by IFS and C4H. The Plant Journal **85**, 689-706.

Demidchik V, Shabala S, Isayenkov S, Cuin TA, Pottosin I. 2018. Calcium transport across plant membranes: mechanisms and functions. New Phytologist 220: 49-69.

Do TD, Chen H, Hien VTT, *et al.* 2016. Ncl synchronously regulates Na^+, K^+, and Cl^- in soybean and greatly increases the grain yield in saline field conditions. Scientific Reports **6**, 19147.

Dong W, Wang M, Xu F, Quan T, Peng K, Xiao L, Xia G. 2013. Wheat oxophytodienoate reductase gene TaOPR1 confers salinity tolerance via enhancement of abscisic acid signaling and reactive oxygen species scavenging. Plant Physiology **161**, 1217-1228.

Du Z, Zhou X, Ling Y, Zhang Z, Su Z. 2010. agriGO: a GO analysis toolkit for the agricultural community. Nucleic Acids Research **38**, 64-70.

Choudhury FK, Rivero RM, Blumwald E, Mittler R. 2017. Reactive oxygen species, abiotic stress and stress combination. The Plant Journal **90**, 856–867.

Flowers TJ, Galal HK, Bromham L. 2010. Evolution of halophytes: multiple origins of salt tolerance in land plants. Functional Plant Biology **37**, 604-612.

Foreman J, Demidchik V, Bothwell JH, *et al*. 2003. Reactive oxygen species produced by NADPH oxidase regulate plant cell growth. Nature **422**, 442-446.

Foyer CH, Noctor G. 2005. Redox homeostasis and antioxidant signaling: a metabolic interface between stress perception and physiological responses. Plant Cell **17**, 1866-1875.

Gao X, Brodhagen M, Isakeit T, Brown SH, Göbel C, Betran J, Feussner I, Keller NP, Kolomiets MV. 2009. Inactivation of the lipoxygenase ZmLOX3 increases susceptibility of maize to *Aspergillus spp*. Molecular Plant Microbe Interact **22**, 222–231

Ge Y, Li Y, Zhu YM, Bai X, Lv DK, Guo D, Ji W, Cai H. 2010. Global transcriptome profiling of wild soybean *Glycine soja* roots under $NaHCO_3$ treatment. BMC Plant Biology **10**, 153.

Gill SS, Tuteja N. 2010. Reactive oxygen species and antioxidant machinery in abiotic stress tolerance in crop plants. Plant Physiology and Biochemistry **48**, 909-930.

Gilliham M, Able JA, Roy SJ. 2017. Translating knowledge about abiotic stress tolerance to breeding programmes. The Plant Journal **90**, 898-917.

Grant D, Nelson RT, Cannon SB, Shoemaker RC. 2010. SoyBase, the USDA-ARS soybean genetics and genomics database. Nucleic Acids Research **38**, D843-6.

Gribskov M, McLachlan AD, Eisenberg D. 1987. Profile analysis: detection of distantly related proteins. Proceedings of the National Academy of Sciences USA **84**, 4355-4358.

Guan R, Qu Y, Guo Y, *et al*. 2014. Salinity tolerance in soybean is modulated by natural variation in GmSALT3. The Plant Journal **80**, 937-950.

Guttikonda SK, Trupti J, Bisht NC, Chen H, An YQC, Pandey S, Xu D, Yu O. 2010. Whole genome co-expression analysis of soybean cytochrome P450 genes identifies nodulation-specific P450 monooxygenases. BMC Plant Biology **10**, 243.

Hosmani PS, Kamiya T, Danku J, Naseer S, Geldner N, Guerinot ML, Salt DE. 2013. Dirigent domain-containing protein is part of the machinery required for formation of the lignin-based Casparian strip in the root. Proceedings of the National Academy of Sciences USA **11035**, 14498-14503.

Hu R, Fan C, Li H, Zhang Q, Fu YF. 2009. Evaluation of putative reference genes for gene expression normalization in soybean by quantitative real-time RT-PCR. BMC molecular biology **10**, 93.

Hu T, Hu Z, Zeng H, Qv X, Chen G. 2015. Tomato lipoxygenase D involved in the biosynthesis of jasmonic acid and tolerance to abiotic and biotic stress in tomato. Plant Biotechnology Reports **9**, 37–45.

Jia T, An J, Liu Z, Yu B, Chen J. 2017. Salt stress induced soybean GmIFS1 expression and isoflavone accumulation and salt tolerance in transgenic soybean cotyledon hairy roots and tobacco. Plant Cell, Tissue and Organ Culture **128**, 469-477.

Kamiya T, Borghi M, Wang P, *et al*. 2015. The MYB36 transcription factor orchestrates Casparian strip formation. Proceedings of the National Academy of Sciences USA **11233**, 10533-10538.

Kanehisa M, Araki M, Goto S, *et al*. 2007. KEGG for linking genomes to life and the environment. Nucleic Acids Research **36**, D480-4.

Kim D, Pertea G, Trapnell C, Pimentel H, Kelley R, Salzberg SL. 2013. TopHat2: accurate alignment of transcriptomes in the presence of insertions, deletions and gene fusions. Genome Biology **14**, R36.

Lam HM, Xu X, Liu X, *et al*. 2010. Resequencing of 31 wild and cultivated soybean genomes identifies patterns of genetic diversity and selection. Nature Genetics **42**, 1053-1059.

Langfelder P, Horvath S. 2008.WGCNA: an R package for weighted correlation network analysis. BMC Bioinformatics **91**, 559.

Langfelder P, Zhang B, Horvath S. 2008. Defining clusters from a hierarchical cluster tree: the Dynamic Tree Cut package for R. Bioinformatics **245**, 719–720.

Lee Y, Rubio MC, Alassimone J, Geldner N. 2013. A mechanism for localized lignin deposition in the endodermis. Cell **1532**, 402-412.

Liu Y, Yu L, Qu Y, *et al*. 2016. GmSALT3, which confers improved soybean salt tolerance in the field, increases leaf Cl^- exclusion prior to Na^+ exclusion but does not improve early vigor under salinity. Frontiers in plant science **7**, 1485

Lu Y, Lam H, Pi E, Zhan Q, Tsai S, Wang C, Kwan Y, Ngai S. 2013. Comparative metabolomics in Glycine max and Glycine soja under salt stress to reveal the phenotypes of their offspring. Journal of Agricultural and Food Chemistry **61**, 8711-8721.

Ma W, Berkowitz GA. 2011. Ca^{2+} conduction by plant cyclic nucleotide gated channels and associated signaling components in pathogen defense signal transduction cascades. New Phytologist **190**, 566-572.

Ma W, Smigel A, Verma R, Berkowitz GA. 2009. Cyclic nucleotide gated channels and related signaling components in plant innate immunity. Plant Signaling & Behavior **4**, 277-282.

Mao X, Cai T, Olyarchuk JG, Wei L. 2005. Automated genome annotation and pathway identification using the KEGG Orthology KO as a controlled vocabulary. Bioinformatics **21**, 3787-3793.

Mittler R. 2002. Oxidative stress, antioxidants and stress tolerance. Trends in Plant Science **7**, 405-410.

Mittler R, Vanderauwera S, Gollery M, Van Breusegem F. 2004. Reactive oxygen gene network of plants. Trends in Plant Science **9**, 490-498.

Mizutani M, Ohta D. 2010. Diversification of P450 genes during land plant evolution. Annual Review of Plant Biology **61**, 291-315.

Munns R, Gilliham M. 2015. Salinity tolerance of crops–what is the cost? New Phytologist **208**, 668-673.

Munns R, Tester M. 2008 Mechanisms of salinity tolerance. Annual Review of Plant Biology **59**, 651-681.

Neill S, Desikan R, Hancock J. 2002 Hydrogen peroxide signalling. Current Opinion in Plant Biology **5**, 388-395.

Noctor G, Foyer CH. 1998. Ascorbate and glutathione: keeping active oxygen under control. Annual Review of Plant Biology **49**, 249-279.

Overmyer K, Brosché M, Kangasjärvi J. 2003. Reactive oxygen species and hormonal control of cell death. Trends in Plant Science **8**, 335-342.

Oyekan A, Youseff T, Fulton D, Quilley J, McGiff J. 1999. Renal cytochrome P450 ω-hydroxylase and epoxygenase activity are differentially modified by nitric oxide and sodium chloride. Journal of Clinical Investigation **104**, 1131-7.

Padmanaban S, Chanroj S, Kwak JM, Li X, Ward JM, Sze H. 2007. Participation of endomembrane cation/H^+ exchanger AtCHX20 in osmoregulation of guard cells. Plant Physiology **1441**, 82-93.

Pei ZM, Murata Y, Benning G, Thomine S, Klüsener B, Allen GJ, Grill E, Schroeder JI. 2000. Calcium channels activated by hydrogen peroxide mediate abscisic acid signalling in guard cells. Nature **406**, 731-734.

Pi, E, Qu, L, Hu, J, Huang, Y, Qiu, L, Lu, H, Jiang, B, Liu, C, Peng, T, Zhao, Y. 2016 Mechanisms of soybean roots' tolerances to salinity revealed by proteomic and phosphoproteomic comparisons between two cultivars. Molecular & Cellular Proteomics **15**, 266-288.

Prakash D, Niranjan A, Tewari SK, Pushpangadan P. 2001. Underutilised legumes: potential sources for low-cost protein. International Journal of Food Sciences and Nutrition **52**, 337-341.

Qi X, Li MW, Xie M, *et al*. 2014. Identification of a novel salt tolerance gene in wild soybean by whole-genome sequencing. Nature Communication **5**, 4340.

Qin, J, Gu, F, Liu, *et al*. 2013 Proteomic analysis of elite soybean Jidou17 and its parents using iTRAQ-based quantitative approaches. Proteome Science **11**, 12.

Qu Y, Guan R, Bose J, Henderson SW, Wege S, Qiu L. Gilliham M. 2021. Soybean CHX□type ion transport protein GmSALT3 confers leaf Na^+ exclusion via a root derived mechanism, and Cl^- exclusion via a shoot derived process. Plant, Cell & Environment **44**, 856–869.

Roppolo D, De Rybel B, Tendon VD, *et al*. 2011. A novel protein family mediates Casparian strip formation in the endodermis. Nature **473,** 380-383.

Roy SJ, Negrão S, Tester M. 2014. Salt resistant crop plants. Current Opinion in Biotechnology **26**, 115-124.

Royo J, León J, Vancanneyt G, Albar JP, Rosahl S, Ortego F, Castañera P, Sánchez-Serrano JJ. 1999. Antisense-mediated depletion of a potato lipoxygenase reduces wound induction of proteinase inhibitors and increases weight gain of insect pests. Proceedings of the National Academy of Sciences USA **96**,1146–1151.

Saxena A, Singh P, Yadav DK, *et al*. 2013 Identification of cytochrome P450 heme motif in plants proteome. Plant Omics **6**, 1.

Sharma M, Gupta SK, Deeba F, Pandey V. 2017. Effects of reactive oxygen species on crop productivity: an overview. In: Singh VP, Singh S, Tripathi DK, Prasad SM, Chauhan DK, eds. Revisiting the role of ROS in plants: boon Or bane - revisiting the role of ROS. Chapter 6.

Stephan AB, Schroeder JI. 2014. Plant salt stress status is transmitted systemically via propagating calcium waves. Proceedings of the National Academy of Sciences USA **11117**, 6126-6127.

Toorchi M, Yukawa K, Nouri MZ, Komatsu S. 2009. Proteomics approach for identifying osmotic-stress-related proteins in soybean roots. Peptides **30**, 2108-2117.

Trapnell C, Roberts A, Goff L, *et al*. 2012. Differential gene and transcript expression analysis of RNA-seq experiments with TopHat and Cufflinks. Nature Protocols **7**, 562-578.

Ursache R, Andersen TG, Marhavý P, Geldner N. 2018. A protocol for combining fluorescent proteins with histological stains for diverse cell wall components. Plant Journal **93**, 399-412.

Yan Q, Cui X, Lin S, Gan S, Xing H, Dou D. 2016. GmCYP82A3, a soybean cytochrome P450 family gene involved in the jasmonic acid and ethylene signaling pathway, enhances plant resistance to biotic and abiotic stresses. PloS One **11**, e0162253.

Yun CH, Song M, Ahn T, Kim H. 1996. Conformational change of cytochrome P450 1A2 induced by sodium chloride. Journal of Biological Chemistry **271**, 31312-31316.

Zhou G, Qi J, Ren N, Cheng J, Erb M, Mao B, Lou Y. 2009**. S**ilencing OsHI-LOX makes rice more susceptible to chewing herbivores, but enhances resistance to a phloem feeder. Plant Journal **60**, 638–648

Figure legends

Fig. 1. Treatment, sampling strategy and data analysis.

Fig. 2. Overview of DEGs between NIL-T salt-tolerant and NIL-S salt-sensitive soybean samples at the 0h, 6h, and 3d timepoints under non-saline conditions.

Fig. 3. Overview of DEGs (differentially expressed genes) between salt-stressed and control samples in NIL-T and NIL-S soybeans at 6h and 3d.

Fig. 4. Significantly enriched KEGG (Kyoto Encyclopedia of Genes and Genomes) of all DEGs between salt-stressed and control samples in NIL-T and NIL-S soybeans.

Fig. 5 Module - Trait Relationships (MTRs) and corresponding *p*-values (within brackets) between the detected modules on the y-axis and groups (trait) on the x-axis.

Fig. 6 Relative ROS concentrations and enzyme activity of the superoxide anion (O_2^-) scavenger assay in soybean roots.

Table 1. Reads mapping and quality of sequencing for 30 *Glycine max* root samples.

Table 2. GO term analysis of uniquely up- and down-regulated genes under salt treatment in soybean roots at 6h.

Table 3. GO term analysis of uniquely up- and down-regulated genes under salt treatment in soybean roots at 3d.

Table 4. Up-regulated genes in oxidation reduction and oxidoreductase activity GO terms of 3 days salt-treated NIL-T roots. Annotations are achieved from https://www.soybase.org/genomeannotation/.

Table 5 Significant Gene Ontology (GO) terms in MEdeeppink and MEantiquewhite2 modules.

1 Figures

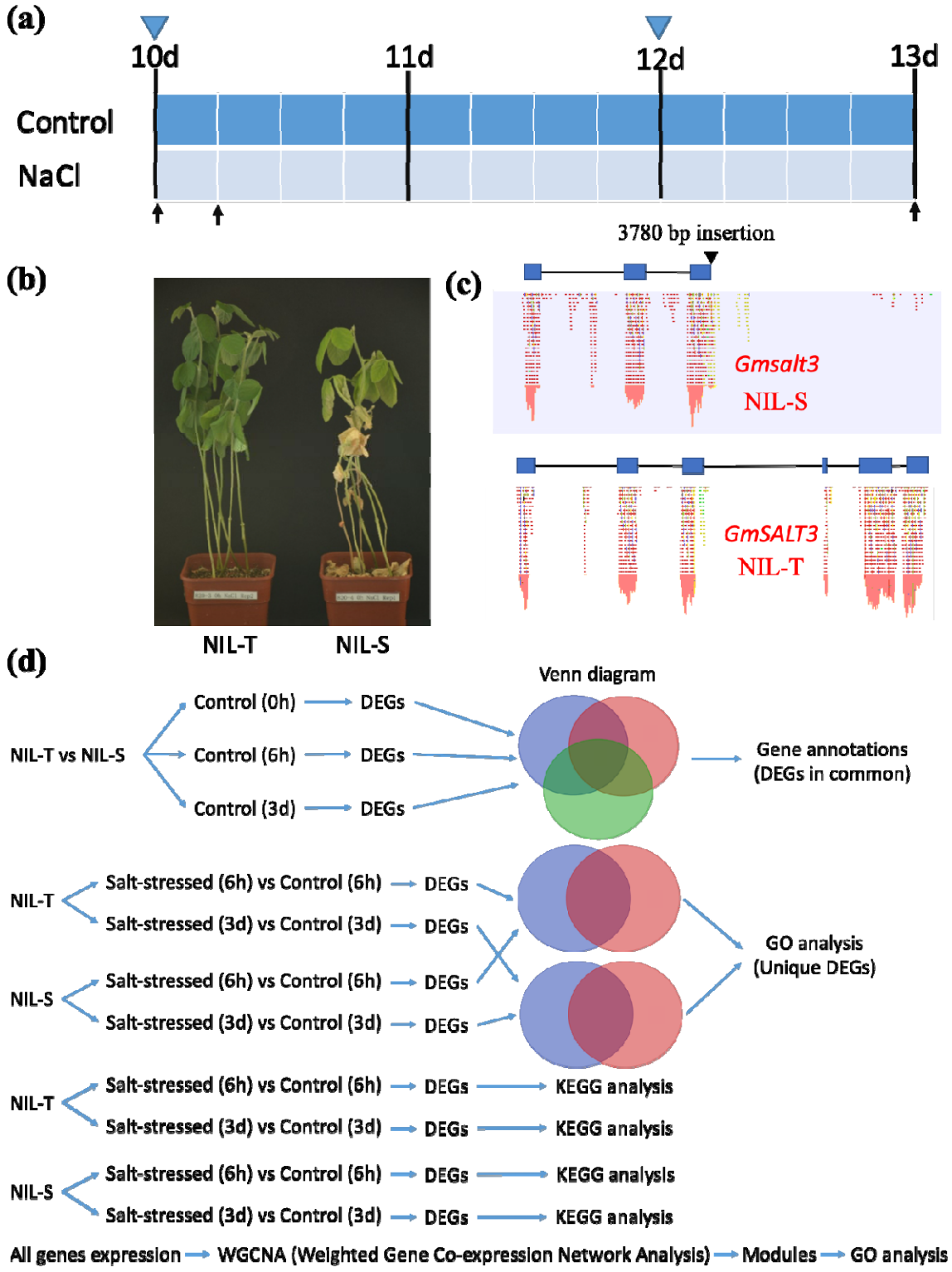

2

3 **Fig. 1. Treatment, sampling strategy and data analysis.** (a) Soybean seedlings were

4 treated with 200 mM NaCl (salt treatment) or water (control) at 10 days after sowing (DAS).

Arrows mean the sampling time points (0h, 6h, 3d), triangle indicated the time point when water or NaCl solution was applied. (b) Pictures of soybean that had been treated with NaCl solution for 11 days. (c) Mapped-reads to *GmSALT3* (bottom) and *Gmsalt3* (above). (d) Flowchart of data analysis. NIL-T, NIL with *GmSALT3* allele; NIL-S, NIL with *Gmsalt3* allele; DEGs, differentially expressed genes; GO, gene ontology.

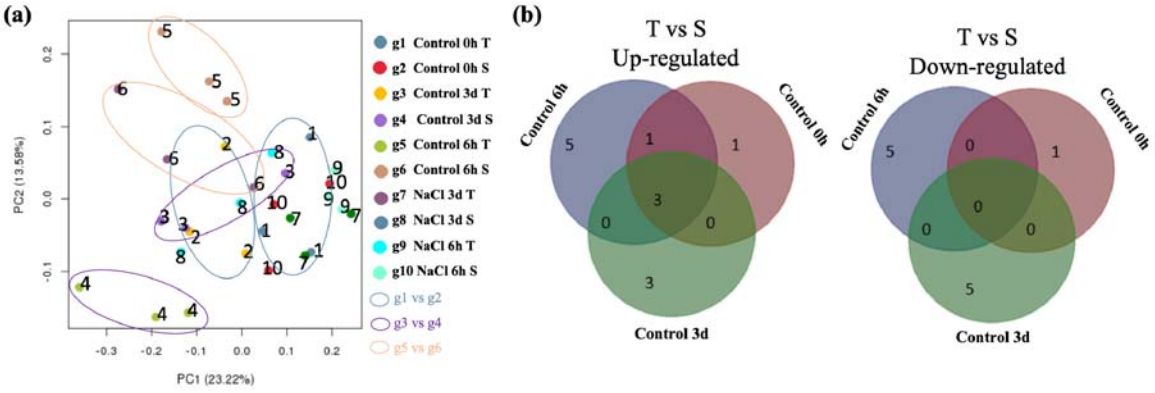

(c)

Gene ID	Annotation	GO terms	Arabidopsis homolog	Arabidopsis annotation
Glyma07g31660	PREDICTED: linoleate 13S-lipoxygenase 3-1, chloroplastic-like [Glycine max]	Biological Process: fatty acid biosynthetic process (GO:0006633); Cellular Component: chloroplast (GO:0009507); Molecular Function: oxidoreductase activity, acting on single donors with incorporation of molecular oxygen, incorporation of two atoms of oxygen (GO:0016702);metal ion binding (GO:0046872).	At1g17420	Lipoxygenase 3
Glyma10g28410	PREDICTED: uncharacterized protein LOC100780872 [Glycine max]	--	At2g37860	Protein of unknown function. Mutants have pale leaves, lower cell density
Glyma20g23930	PREDICTED: 3-hydroxybenzoate 6-hydroxylase 1-like [Glycine max]	Molecular Function: monooxygenase activity (GO:0004497); oxidoreductase activity (GO:0016491); Biological Process: response to stress (GO:0006950); response to abiotic stimulus (GO:0009628); cellular metabolic process (GO:0044237); single-organism metabolic process (GO:0044710); oxidation-reduction process (GO:0055114). Cellular Component: chloroplast (GO:0009507); response to abiotic stimulus (GO:0009628).	At5g05320	FAD/NAD(P)-binding oxidoreductase family protein

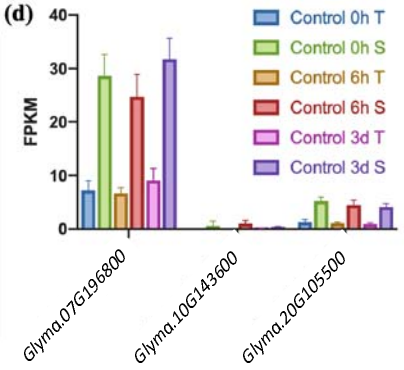

Fig. 2. Overview of DEGs between NIL-T salt-tolerant and NIL-S salt-sensitive soybean samples at the 0h, 6h, and 3d timepoints under non-saline conditions. (a) PCA plot of ten groups (g1 – g10). Different coloured dots represent replicates in each group, different coloured circles represent comparisons between groups (g1 vs g2, g3 vs g4, g5 vs g6). (b) Venn diagram of up- and down-regulated DEGs in NIL-S soybeans at 0h, 6h, and 3d under control conditions. **(**c) Three up-regulated DEGs in NIL-S soybeans at all 0h, 6h, and 3d under control conditions, and their expression profile is shown in (d). The cutoffs for DEGs are Log_2FC (fold change) ≥ 1, FDR (False Discover Rate) < 0.01.

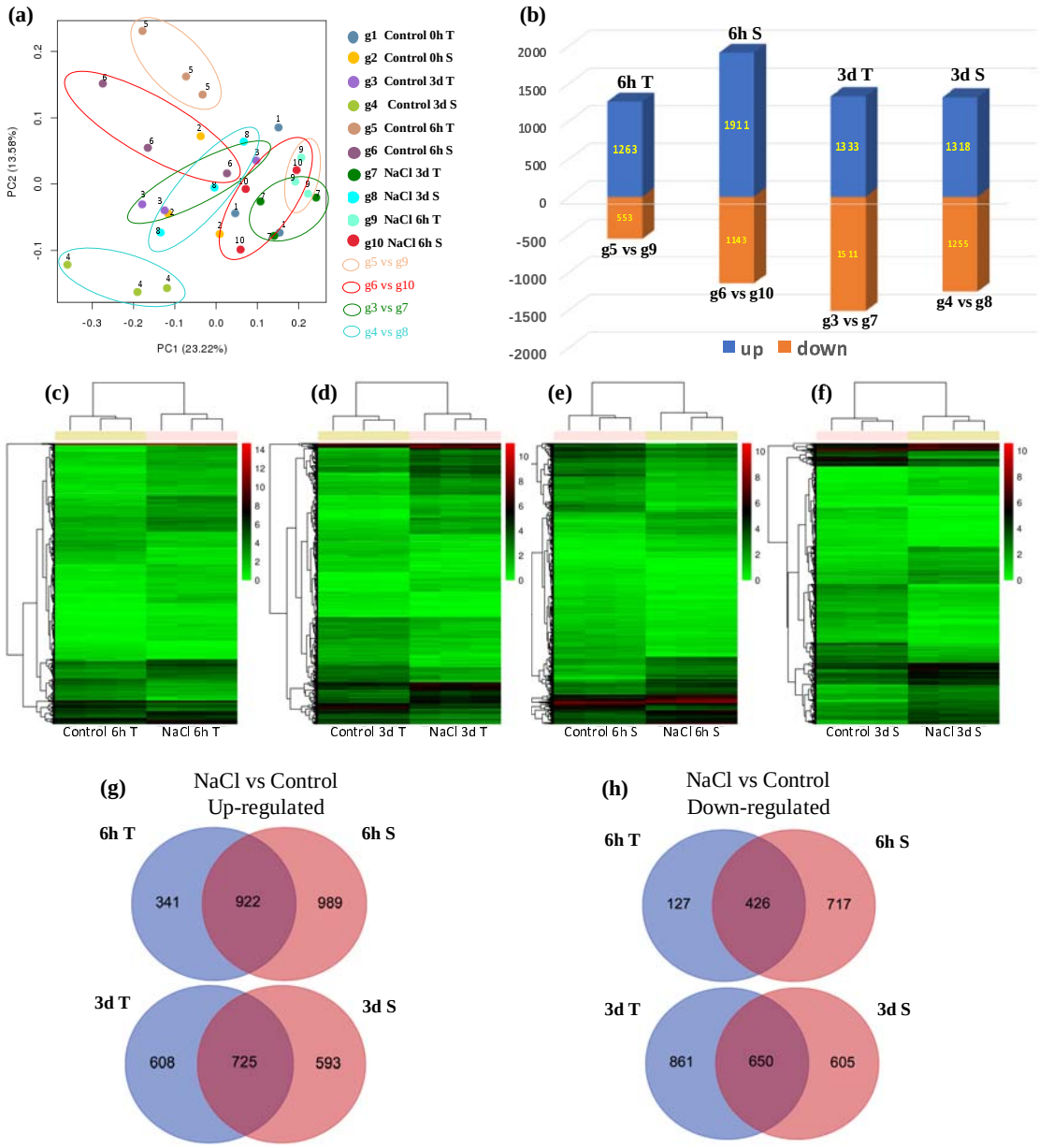

Fig. 3. Overview of DEGs (differentially expressed genes) between salt-stressed and control samples in NIL-T and NIL-S soybeans at 6h and 3d. (a) PCA plot of ten groups (g1 – g10). Different coloured dots represent replicates in each group, different coloured circles represent comparisons between groups (g5 vs g9, g6 vs g10, g3 vs g7, g4 vs g8). (b) Numbers of DEGs (up- and down-regulated) between groups. Clustering of DEGs in log_2FPKMs (Fragments Per Kilobase of transcript per Million) of group 3 to 10 (c-f). The false colour scale from green through to red indicates increasing log_2FPKM. (g) Venn diagram of up-regulated DEGs in NIL-T and NIL-S soybeans at 6h and 3d under NaCl treatment. (h) Venn diagram of down-regulated DEGs in NIL-T and NIL-S soybeans at 6h

and 3d under NaCl treatment. The cut-offs for DEGs are Log_2FC (fold change) ≥ 1, FDR (False Discover Rate) < 0.01.

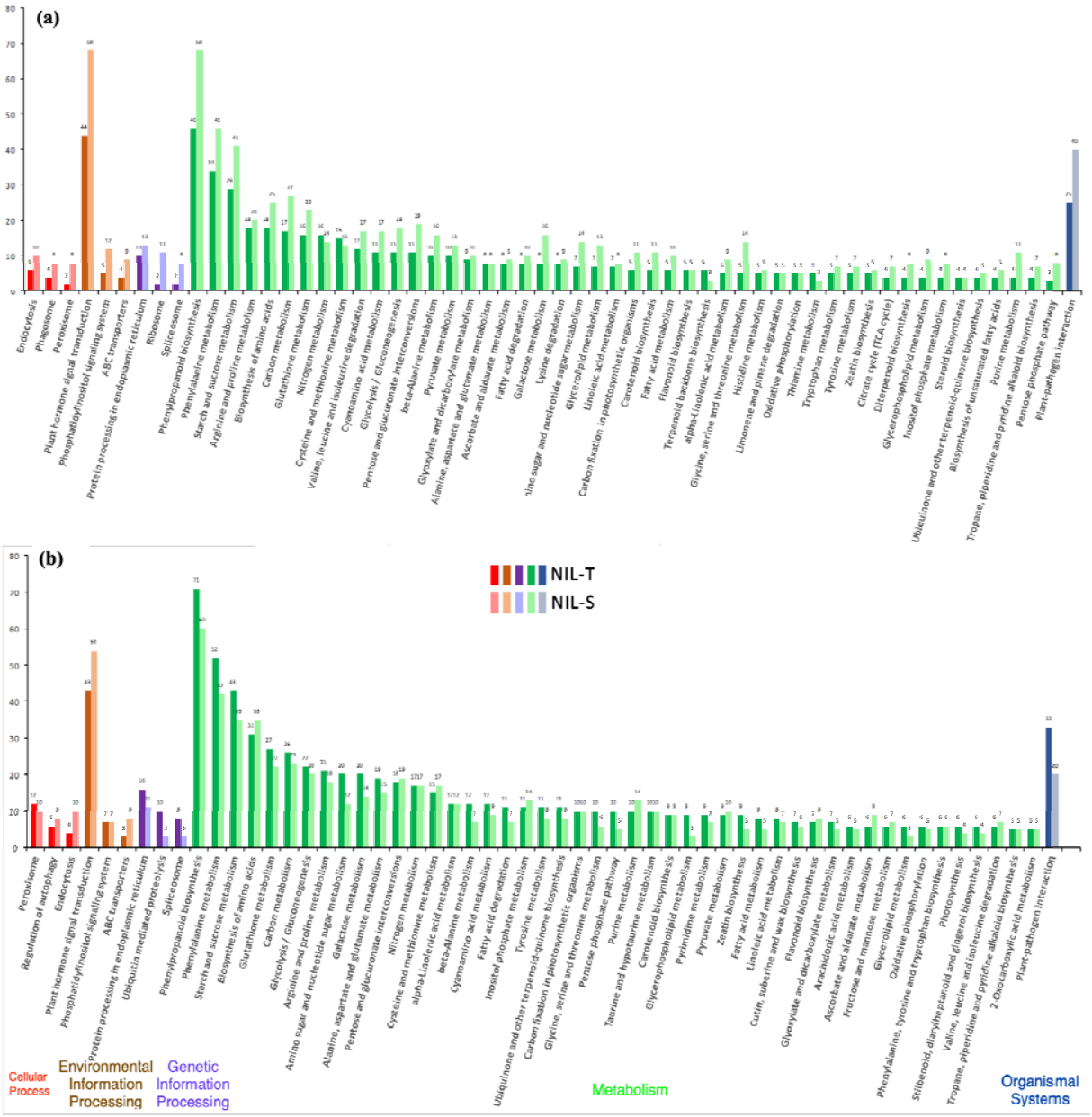

Fig. 4. Significantly enriched KEGG (Kyoto Encyclopedia of Genes and Genomes) of all DEGs between salt-stressed and control samples in NIL-T and NIL-S soybeans. a 6h KEGG enrichment. **b** 3d KEGG enrichment. KEGG enrichment *P*-value cut-off ≤ 0.05.

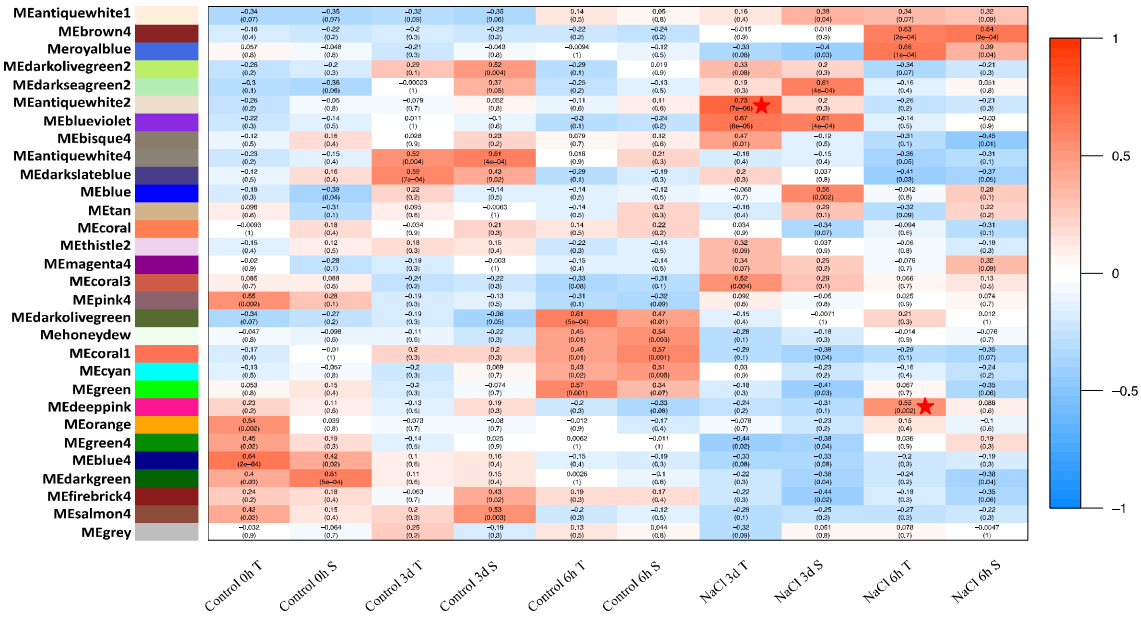

Fig. 5 Module - Trait Relationships (MTRs) and corresponding *p*-values (within brackets) between the detected modules on the y-axis and groups (trait) on the x-axis. The MTRs are coloured based on their correlation: from red (strong positive correlation) to blue (strong negative correlation). Each group contains three biological replicates. Pentagram represents modules of interest.

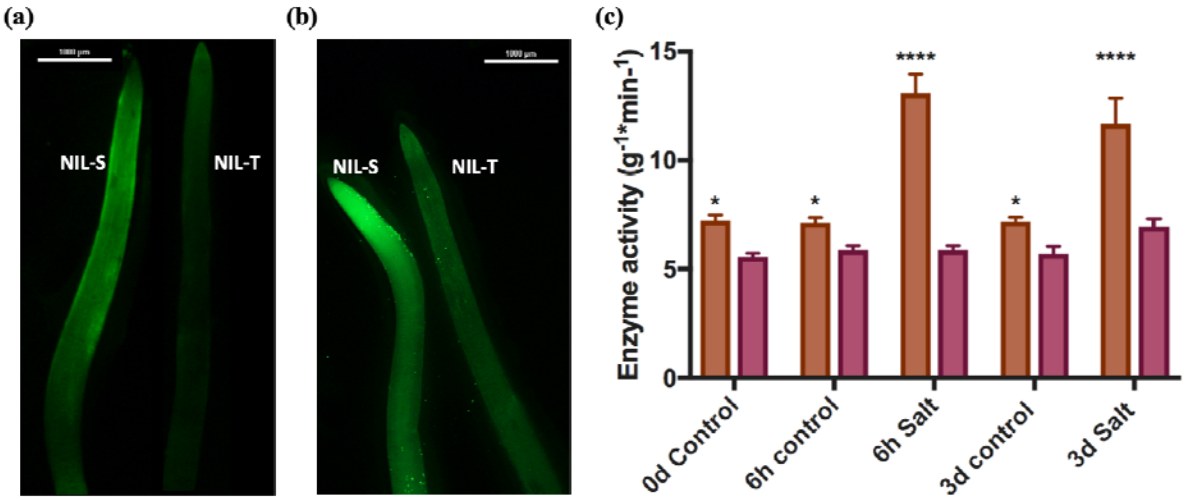

Fig. 6 Relative ROS concentrations and enzyme activity of the superoxide anion (O_2^-) scavenger assay in soybean roots. NIL-T and NIL-S were labelled with 30 μM DCFDA for 10 min under control conditions (a) and with salt treatment for 3 days (b). Green fluorescence indicates the presence of ROS. (c) scavenging activity of the superoxide anion (O_2^-) of NIL-T (brown) and NIL-S (red) with or without salt treatment. Asterisk indicates a significant difference between NIL-T and NIL-S at *P <0.05 ****P<0.0001.

Table 1. Reads mapping and quality of sequencing for 30 *Glycine max* root samples.

Group	Sample	Total Reads	Mapped Reads	Clean reads	Clean bases	GC Content	%≥Q30
g1	Control 0h T1	57,699,406	49,137,608 (85.16%)	28,849,703	7,212,425,750	50.56%	92.05%
	Control 0h T2	59,769,628	51,025,677 (85.37%)	29,884,814	7,471,203,500	52.37%	93.30%
	Control 0h T3	62,070,060	53,862,681 (86.78%)	31,035,030	7,758,757,500	50.01%	93.35%
g2	Control 0h S1	43,642,298	32,134,039 (73.63%)	21,821,149	5,455,287,250	48.70%	88.44%
	Control 0h S2	46,423,344	39,574,288 (85.25%)	23,211,672	5,802,918,000	49.23%	94.08%
	Control 0h S3	56,017,714	43,638,938 (77.90%)	28,008,857	7,002,214,250	50.34%	93.88%
g3	Control 3d T1	48,501,908	42,642,939 (87.92%)	24,250,954	6,062,738,500	48.90%	93.69%
	Control 3d T2	60,432,732	53,220,906 (88.07%)	30,216,366	7,554,091,500	50.86%	94.28%
	Control 3d T3	48,809,732	41,680,164 (85.39%)	24,404,866	6,101,216,500	48.29%	92.51%
g4	Control 3d S1	47,058,528	39,937,443 (84.87%)	23,529,264	5,882,316,000	48.39%	93.58%
	Control 3d S2	48,461,144	40,928,669 (84.46%)	24,230,572	6,057,643,000	47.83%	94.18%
	Control 3d S3	49,796,814	40,986,303 (82.31%)	24,898,407	6,224,601,750	50.35%	94.30%
g5	Control 6h T1	51,648,018	30,700,905 (59.44%)	25,824,009	6,456,002,250	48.37%	84.72%
	Control 6h T2	34,427,522	21,774,315 (63.25%)	17,213,761	4,303,440,250	48.21%	87.04%
	Control 6h T3	84,627,144	55,643,274 (65.75%)	42,313,572	10,578,393,000	48.00%	86.74%
g6	Control 6h S1	62,158,510	50,330,267 (80.97%)	31,079,255	7,769,813,750	48.61%	92.06%
	Control 6h S2	59,768,732	44,180,997 (73.92%)	29,884,366	7,471,091,500	48.12%	89.44%
	Control 6h S3	48,852,622	41,445,404 (84.84%)	24,426,311	6,106,577,750	49.05%	93.76%
g7	NaCl 3d T1	47,478,210	39,318,129 (82.81%)	23,739,105	5,934,776,250	49.12%	93.71%
	NaCl 3d T2	49,524,852	42,007,601 (84.82%)	24,762,426	6,190,606,500	50.44%	94.94%
	NaCl 3d T3	53,918,342	45,880,121 (85.09%)	26,959,171	6,739,792,750	52.93%	93.81%
g8	NaCl 3d S1	55,228,034	45,771,588 (82.88%)	27,614,017	6,903,504,250	47.24%	92.28%
	NaCl 3d S2	57,398,436	46,291,922 (80.65%)	28,699,218	7,174,804,500	48.58%	92.30%
	NaCl 3d S3	58,773,304	47,497,496 (80.81%)	29,386,652	7,346,663,000	48.48%	91.31%
g9	NaCl 6h T1	53,174,654	45,735,099 (86.01%)	26,587,327	6,646,831,750	51.47%	93.56%
	NaCl 6h T2	52,045,484	43,779,481 (84.12%)	26,022,742	6,505,685,500	50.75%	93.30%
	NaCl 6h T3	55,579,826	45,167,976 (81.27%)	27,789,913	6,947,478,250	51.54%	92.62%
g10	NaCl 6h S1	54,197,662	45,095,587 (83.21%)	27,098,831	6,774,707,750	48.34%	92.64%
	NaCl 6h S2	53,274,670	45,180,893 (84.81%)	26,637,335	6,659,333,750	50.44%	92.49%
	NaCl 6h S3	47,601,546	40,826,998 (85.77%)	23,800,773	5,950,193,250	48.16%	94.75%

Table 2. GO term analysis of uniquely up- and down-regulated genes under salt treatment in soybean roots at 6h. (a) Up-regulated genes in NIL-T soybean roots. (b) Up-regulated genes in NIL-S soybean roots. (c) Down-regulated genes in NIL-T soybean roots. (d) Down-regulated genes in NIL-S soybean roots. CC, Cellular Component; BP, Biological Process; MF, Molecular Function.

(a)

GO term	Ontology	Description	Number in input list	Number in BG/Ref	p-value	FDR
GO:0009607	BP	response to biotic stimulus	7	64	9.3e-08	2.4e-05
GO:0006952	BP	defense response	7	118	4.4e-06	0.00056
GO:0055114	BP	oxidation reduction	28	2408	6.1e-05	0.0051
GO:0005507	MF	copper ion binding	9	219	3.4e-06	0.00071
GO:0016491	MF	oxidoreductase activity	32	2744	1.5e-05	0.0016
GO:0004866	MF	endopeptidase inhibitor activity	5	92	0.00016	0.0083

(b)

GO term	Ontology	Description	Number in input list	Number in BG/Ref	p-value	FDR
GO:0006355	BP	regulation of transcription, DNA-dependent	69	1874	2e-05	0.0016

(c)

GO term	Ontology	Description	Number in input list	Number in BG/Ref	p-value	FDR
GO:0016021	CC	integral to membrane	11	1419	0.00065	0.0058

(d)

GO term	Ontology	Description	Number in input list	Number in BG/Ref	p-value	FDR
GO:0020037	MF	heme binding	23	728	8e-05	0.012
GO:0009055	MF	electron carrier activity	21	702	0.00033	0.018
GO:0004190	MF	aspartic-type endopeptidase activity	9	169	0.00042	0.018
GO:0015035	MF	protein disulfide oxidoreductase activity	7	96	0.00031	0.018

Table 3. GO term analysis of uniquely up- and down-regulated genes under salt treatment in soybean roots at 3d. (a) Up-regulated genes in NIL-T soybean roots. (b) Up-regulated genes in NIL-S soybean roots. (c) Down-regulated genes in NIL-T soybean roots. (d) Down-regulated genes in NIL-S soybean roots. CC, Cellular Component; BP, Biological Process; MF, Molecular Function.

(a)

GO term	Ontology	Description	Number in input list	Number in BG/Ref	p-value	FDR
GO:0055114	BP	oxidation reduction	53	2408	8.9e-06	0.0037
GO:0016491	MF	oxidoreductase activity	57	2744	2e-05	0.0073

(b)

GO term	Ontology	Description	Number in input list	Number in BG/Ref	p-value	FDR
GO:0006355	BP	regulation of transcription, DNA-dependent	51	1874	9.8e-08	3.6e-06
GO:0006468	BP	protein amino acid phosphorylation	45	2356	0.002	0.023
GO:0048544	BP	recognition of pollen	14	135	3.8e-09	3e-07
GO:0015743	BP	malate transport	5	34	0.0001	0.0013

(c)

GO term	Ontology	Description	Number in input list	Number in BG/Ref	p-value	FDR
GO:0007018	BP	microtubule-based movement	17	155	9.8e-09	5.2e-06
GO:0003777	MF	microtubule motor activity	17	155	9.8e-09	2.4e-06
GO:0043531	MF	ADP binding	27	467	2.1e-07	2e-05
GO:0004565	MF	beta-galactosidase activity	6	37	9.5e-05	0.0031
GO:0017171	MF	serine hydrolase activity	17	330	0.00014	0.0041
GO:0009341	CC	beta-galactosidase complex	6	37	9.5e-05	0.009

(d)

GO term	Ontology	Description	Number in input list	Number in BG/Ref	p-value	FDR
GO:0055085	BP	transmembrane transport	29	1167	1.9e-05	0.0075
GO:0022857	MF	transmembrane transporter activity	24	1020	0.00022	0.036

Table 4. Up-regulated genes in oxidation reduction and oxidoreductase activity GO terms of 3 days salt-treated NIL-T roots. Annotations are achieved from https://www.soybase.org/genomeannotation/.

Gmax2.0 Protein ID	Control 3d T3 (FPKM)	NaCl 3d T3 (FPKM)	PFAM_Descriptions	Panther_Descriptions	KOG_Descriptions
Glyma.13G104100	0.003926	1.178719	Flavin-containing amine oxidoreductase	AMINE OXIDASE	Flavin-containing amine oxidase
Glyma.01G210400	0.200688	2.578006	alpha/beta-C-terminal domain; L-lactate/malate dehydrogenase, NAD binding domain'	MALATE/ANY DUCTATE DEHYDROGENASE	Lactate dehydrogenase
Glyma.11G024100	0.040890	1.424517	Glutathione peroxidase	GLUTATHIONE PEROXIDASE	Glutathione peroxidase
Glyma.13G173500	71.332430	279.415321	Cytochrome P450	FAMILY NOT NAMED	Cytochrome_P450_CYP2_subfamily
Glyma.02G202500	0.297011	0.974227	Aldehyde dehydrogenase family	ALDEHYDE DEHYDROGENASE-RELATED	Aldehyde_dehydrogenase
Glyma.18G211000	1.800717	5.575660	Peroxidase	NA	NA
Glyma.16G179200	1.461360	2.027147	CobQ/CobB/MinD/ParA nucleotide binding domain	FAMILY NOT NAMED	Predicted_ATPase,_nucleotide-binding
Glyma.06G137000	0.370632	1.164678	2OG-Fe(II) oxygenase superfamily	OXIDOREDUCTASE, 2OG-FE(II) DIOXYGENASE FAMILY	Iron/ascorbate_family_oxidoreductases
Glyma.14G099000	3.113720	7.206253	Cytokinin dehydrogenase 1, FAD and cytokinin binding; FAD binding domain	D-LACTATE DEHYDROGENASE	Proteins_containing_the_FAD_binding_domain
Glyma.16G021200	6.619380	14.499433	Cytochrome P450	FAMILY NOT NAMED	Cytochrome_P450_CYP2_subfamily
Glyma.05G214000	27.504467	64.849500	NAD binding domain of 6-phosphogluconate dehydrogenase	6-PHOSPHOGLUCONATE DEHYDROGENASE	6-phosphogluconate_dehydrogenase
Glyma.11G175900	6.988560	13.550913	Cytochrome P450	FAMILY NOT NAMED	Cytochrome_P450_CYP4/CYP19/CYP26_subfamilies
Glyma.17G225700	1.988862	5.125209	FAD binding domain; Cytokinin dehydrogenase 1, FAD and cytokinin binding'	D-LACTATE DEHYDROGENASE	Proteins_containing_the_FAD_binding_domain
Glyma.04G123800	1.602680	3.730430	Alternative oxidase	NA	NA
Glyma.19G123800	0.464332	1.785490	Ruberythrin	NA	NA
Glyma.08G303800	6.717425	16.957918	Flavin-containing amine oxidoreductase	AMINE OXIDASE	Amine_oxidase
Glyma.07G168500	10.873917	21.774467	2OG-Fe(II) oxygenase superfamily	OXIDOREDUCTASE, 2OG-FE(II) DIOXYGENASE FAMILY	Iron/ascorbate_family_oxidoreductases
Glyma.09G132300	0.903153	1.607179	CobQ/CobB/MinD/ParA nucleotide binding domain	FAMILY NOT NAMED	Predicted_ATPase,_nucleotide-binding
Glyma.01G056100	0.352736	0.825042	2OG-Fe(II) oxygenase superfamily	OXIDOREDUCTASE, 2OG-FE(II) DIOXYGENASE FAMILY	Iron/ascorbate_family_oxidoreductases
Glyma.18G177000	3.020740	6.342210	Zinc-binding dehydrogenase; Alcohol dehydrogenase GroES-like domain'	ALCOHOL DEHYDROGENASE RELATED	Alcohol_dehydrogenase,_class_V
Glyma.03G008100	0.296423	0.491798	Cytochrome P450	FAMILY NOT NAMED	Cytochrome_P450_CYP4/CYP19/CYP26_subfamilies
Glyma.05G041200	0.140178	0.587665	Ferric reductase NAD binding domain; FAD-binding domain'	NADPH OXIDASE	NA
Glyma.03G098600	3.067300	7.794463	Zinc-binding dehydrogenase	ALCOHOL DEHYDROGENASE RELATED	Predicted_NAD-dependent_oxidoreductase
Glyma.17G167200	3.871524	8.781803	FAD dependent oxidoreductase	FAD/NAD BINDING OXIDOREDUCTASES	Possible_oxidoreductase
Glyma.17G054500	0.337715	0.774757	FAD binding domain; Cytokinin dehydrogenase 1, FAD and cytokinin binding'	GULONOLACTONE OXIDASE	Proteins_containing_the_FAD_binding_domain
Glyma.03G122000	26.622283	34.891684	Cytochrome P450	FAMILY NOT NAMED	Cytochrome_P450_CYP2_subfamily
Glyma.20G169200	30.460700	53.630300	Peroxidase	NA	NA
Glyma.11G185700	6.940457	9.682720	Cytochrome P450	FAMILY NOT NAMED	Cytochrome_P450_CYP4/CYP19/CYP26_subfamilies
Glyma.06G113500	0.626838	1.859539	Phosphorhistidine phosphatase; Rieske [2Fe-2S] domain'	IRON-SULFUR DOMAIN CONTAINING PROTEIN	NA
Glyma.15G071000	14.283107	37.916700	Polyphenol oxidase middle domain; Common central domain of tyrosinase'	TYROSINASE	NA
Glyma.10G231200	6.984682	16.091238	Fatty acid hydroxylase superfamily	NA	NA
Glyma.10G200800	1.982207	2.714897	Cytochrome P450	FAMILY NOT NAMED	Cytochrome_P450_CYP2_subfamily
Glyma.15G129200	8.068280	20.633733	Peroxidase	NA	NA
Glyma.13G168700	4.586266	11.779662	catalytic domain; D-isomer specific 2-hydroxyacid dehydrogenase, NAD binding	2-HYDROXYACID DEHYDROGENASE-RELATED	Glyoxylate/hydroxypyruvate_reductase_(D-isomer-
Glyma.10G041800	0.537806	1.160858	Flavin-binding monooxygenase-like	DIMETHYLANILINE MONOOXYGENASE	Flavin-containing_monooxygenase
Glyma.17G015400	4.400850	6.387743	Cytochrome P450	FAMILY NOT NAMED	Cytochrome_P450_CYP2_subfamily
Glyma.19G126000	35.728733	48.534900	Cytochrome P450	FAMILY NOT NAMED	Cytochrome_P450_CYP2_subfamily
Glyma.02G052700	14.152725	29.022591	Peroxidase	NA	NA
Glyma.09G218700	1.588015	2.484951	High-affinity nickel-transport protein	NA	NA
Glyma.06G017900	12.309302	24.021127	Catalase; Catalase-related immune-responsive'	CATALASE	Catalase
Glyma.12G107000	7.262499	15.171104	Pyridine nucleotide-disulphide oxidoreductase; Pyridine nucleotide-disulphide	NADH DEHYDROGENASE-RELATED	NADH-dehydrogenase_(ubiquinone)
Glyma.11G149100	0.525827	1.166289	FAD binding domain; Cytokinin dehydrogenase 1, FAD and cytokinin binding'	GULONOLACTONE OXIDASE	Proteins_containing_the_FAD_binding_domain
Glyma.20G192200	0.856669	1.672531	Lactate/malate dehydrogenase, alpha/beta C-terminal domain; Lactate/malate	MALATE DEHYDROGENASE	Malate_dehydrogenase
Glyma.18G009700	43.848325	60.982450	Glyceraldehyde 3-phosphate dehydrogenase, NAD binding domain	GLYCERALDEHYDE 3-PHOSPHATE	Glyceraldehyde_3-phosphate_dehydrogenase
Glyma.06G302700	12.621392	25.677667	Peroxidase	NA	NA
Glyma.11G122700	29.647954	50.738974	Cytochrome P450	NA	Cytochrome_P450_CYP4/CYP19/CYP26_subfamilies
Glyma.05G207100	36.391806	79.784041	Glutathione peroxidase	GLUTATHIONE PEROXIDASE	Glutathione_peroxidase
Glyma.08G033400	19.221367	37.310567	NAD binding domain of 6-phosphogluconate dehydrogenase	3-HYDROXYISOBUTYRATE DEHYDROGENASE-	Predicted_dehydrogenase
Glyma.20G183100	0.857535	1.409998	FAD dependent oxidoreductase	GLYCEROL-3-PHOSPHATE DEHYDROGENASE	Glycerol-3-phosphate_dehydrogenase
Glyma.02G149900	1.938657	3.676737	2OG-Fe(II) oxygenase superfamily	NA	Uncharacterized_conserved_protein
Glyma.08G226600	1.010831	1.571265	Complex I intermediate-associated protein 30 (C1QA30); NmrA-like family'	NAD DEPENDENT EPIMERASE/DEHYDRATASE	Predicted_dehydrogenase
Glyma.14G205200	91.015528	123.589510	Cytochrome P450	FAMILY NOT NAMED	Cytochrome_P450_CYP2_subfamily
Glyma.15G019300	25.004079	60.218292	Malic enzyme, N-terminal domain; Malic enzyme, NAD binding domain'	MALIC ENZYME-RELATED	NADP+-dependent_malic_enzyme

Table 5 Significant Gene Ontology (GO) terms in MEdeeppink and MEantiquewhite2 modules. (a) Enriched GO terms in MEdeeppink module (NIL-T after 6h salt treatment); (b) Enriched GO terms in MEantiquewhite2 module (NIL-T after 3d salt treatment). C, Cellular Component; P, Biological Process; F, Molecular Function.

(a)

GO term	Ontology	Description	Number in input list	Number in BG/Ref	p-value	FDR
GO:0005886	C	plasma membrane	12	81	5.00E-20	1.70E-18
GO:0031224	C	intrinsic to membrane	12	1453	4.40E-06	4.90E-05
GO:0016021	C	integral to membrane	12	1419	3.50E-06	4.90E-05
GO:0044425	C	membrane part	13	1801	7.00E-06	5.80E-05
GO:0016020	C	membrane	15	3518	0.00053	0.0035

(b)

GO term	Ontology	Description	Number in input list	Number in BG/Ref	p-value	FDR
GO:0009207	P	purine ribonucleoside triphosphate catabolic process	6	40	0.0000092	0.00044
GO:0046907	P	intracellular transport	14	297	0.0000073	0.00044
GO:0016567	P	protein ubiquitination	9	130	0.000019	0.00076
GO:0046034	P	ATP metabolic process	5	46	0.00021	0.0046
GO:0046578	P	regulation of Ras protein signal transduction	6	91	0.00061	0.011
GO:0004674	F	protein serine/threonine kinase activity	14	39	3.1E-16	1.2E-13
GO:0046872	F	metal ion binding	65	3600	0.000024	0.0021
GO:0042623	F	ATPase activity, coupled	12	343	0.00047	0.021
GO:0030120	C	vesicle coat	5	41	0.00013	0.0013
GO:0031981	C	nuclear lumen	5	105	0.0066	0.039
GO:0016021	C	integral to membrane	26	1419	0.0068	0.039